STUDY ON ENERGY STABILITY OF HIGH-CHARGE BUNCHES FROM LASER PLASMA ACCELERATORS FOR RING INJECTION

Y. Shi[1,2], X. Shi[*,1], H. Xu[†,1,2]
[1]Institute of High Energy Physics, Chinese Academy of Sciences, 100049 Beijing, China
[2]University of Chinese Academy of Sciences, 100049 Beijing, China

Abstract

Laser plasma accelerators (LPAs) offer accelerating gradients several orders of magnitude higher than conventional RF accelerators, enabling compact high-energy accelerator designs. However, LPA-generated electron beams typically exhibit large energy spread and significant shot-to-shot energy jitter, especially at high charge, which limits their use in applications such as ring injectors.

Our previous work proposed a transfer line integrating an active plasma dechirper (APD), a passive plasma dechirper (PPD), and magnetic chicanes, achieving reductions of energy jitter from ±2% to 0.1% and energy spread from 1.2% to 0.5% for 500 pC beams (Xueyan Shi *et al.*, New J. Phys. 26, 073045, 2024).

In this work, we extend the scheme to the nanocoulomb regime. Start-to-end simulations show that for a 1 nC beam with an initial rms energy spread of 1.2% and energy jitter of ±2%, the optimized configuration reduces these values to 0.4% and ±0.05%, respectively, while maintaining a transmission of ~82%. The results further demonstrate the feasibility of employing LPA beams for HEPS booster injection.

INTRODUCTION

Laser–plasma accelerators (LPAs) can support accelerating gradients exceeding 100 GV/m, far above those of conventional RF cavities, owing to wakefields driven by ultrashort laser–plasma interactions [1–6]. The resulting beams feature ultrashort duration [7], high brightness [8], and low emittance [8–11], making LPAs attractive for ultrafast science and advanced accelerator applications. However, nonlinear injection and acceleration dynamics, together with fluctuations in laser and plasma conditions, lead to substantial shot-to-shot variations in beam energy and energy spread [12], posing challenges for applications requiring high energy stability, such as storage-ring injectors.

To mitigate these fluctuations, both source control and downstream manipulation have been explored. Controlled injection schemes [13, 14] reduce fluctuations at the source, while plasma-based dechirpers effectively suppress energy spread. Passive plasma dechirpers (PPDs) have achieved sub-0.1% energy spread [15], and combinations of magnetic chicanes with active plasma dechirpers (APDs) have demonstrated energy stability approaching 99.9% [16]. Shi *et al.* [17] further showed that introducing an energy chirp via a quadrupole triplet and magnetic chicane, followed by an APD in the linear regime, can reduce the energy spread and jitter of a 50 pC beam from ±2% and 1% to −0.14% ~ +0.04% and 0.24% ~ 0.41%, respectively.

Although these approaches are effective, they are typically limited to tens of pC due to strong beam loading in plasma structures. A subsequent APD–PPD scheme achieved ~ 0.5% energy spread and ~ 0.1% jitter at 500 pC [18], but performance degrades at the nC level, which is required for synchrotron light sources such as the High Energy Photon Source (HEPS).

In this work, we optimize the scheme of Ref. [18] for nC-level beams. By balancing the R_{56} of the first magnetic chicane with the APD plasma density, and reducing the PPD density while enlarging its channel radius to mitigate nonlinear effects, the resulting beam meets the longitudinal acceptance of the HEPS booster. This configuration achieves reduced energy spread and jitter while maintaining a transmission efficiency of ~82%.

PLASMA INJECTOR

At the entrance of the beamline, the LPA beam has a relative energy spread of 1.2% and an energy jitter of ±2%. The rms bunch length is approximately 2 μm, with a bunch charge of 1 nC, corresponding to a peak current of about 250 kA. The normalized rms transverse emittance is 2 mm · mrad. These parameters are representative of high-charge LPA beams.

A schematic layout of the beamline is shown in Fig. 1. The system is designed to simultaneously suppress energy jitter and reduce energy spread, while maintaining acceptable transmission.

The upstream section consists of a magnetic chicane followed by an active plasma dechirper (APD). The chicane introduces a longitudinal dispersion R_{56} that converts energy deviations into longitudinal position shifts, establishing a controlled chirp. The APD then provides an approximately linear wakefield that compensates this chirp, substantially reducing the energy jitter.

At the nC level, however, strong beam loading distorts the APD wakefield (see Fig. 2), introducing nonlinear components that, while still suppressing energy jitter, significantly increase the energy spread. To mitigate this effect, a second stage is added downstream: a magnetic chicane with negative R_{56} followed by a passive plasma dechirper (PPD). The chicane reverses the chirp, and the PPD supplies a decelerating wakefield that reduces the correlated energy spread. This two-stage manipulation brings both energy jitter and energy spread within the HEPS booster requirements.

* shixueyan@ihep.ac.cn
† xuhs@ihep.ac.cn

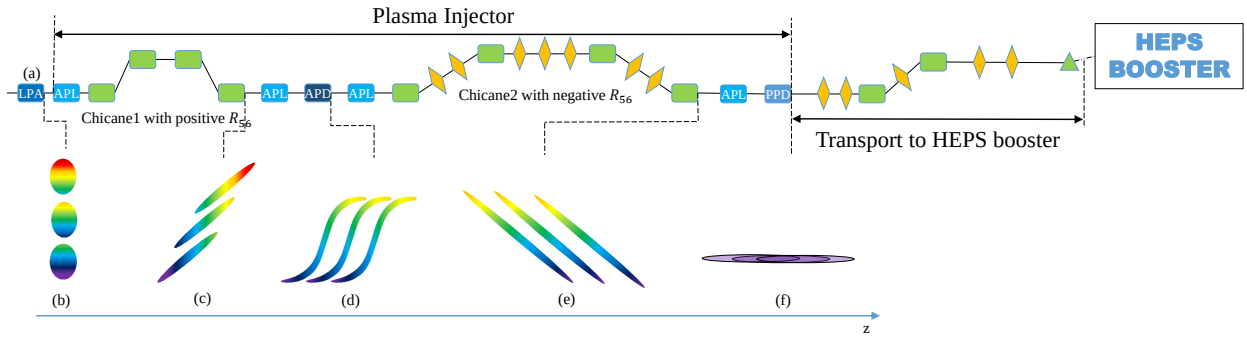

Figure 1: Proposed scheme integrating energy correction and energy-spread reduction within a plasma injector. The beam is first focused by an active plasma lens (APL) and then sent through a magnetic chicane with positive R_{56}, which converts energy jitter into longitudinal position shifts (c). An active plasma dechirper (APD) subsequently provides an approximately linear wakefield to correct the jitter (d). A second chicane with negative R_{56} introduces a reversed chirp (e), after which a passive plasma dechirper (PPD) reduces the correlated energy spread (f). The beam is finally transported to the HEPS booster. Dipoles are shown in blue and quadrupoles in yellow.

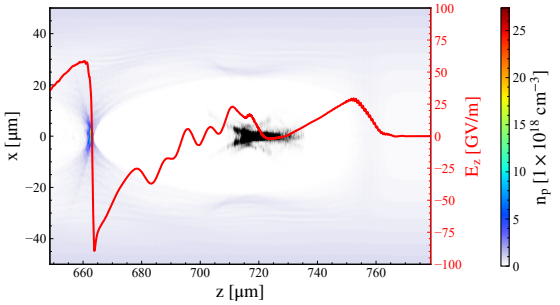

Figure 2: Longitudinal phase space of the beam inside the APD, showing distortion induced by strong beam-loading effects at the nC charge level.

At high charge, the choice of R_{56} in the first chicane and the APD plasma density becomes critical. Increasing R_{56} stretches the bunch and lowers the peak current, easing beam loading, but also requires a longer plasma wavelength to maintain wakefield linearity. Since $\lambda_p\,[\mu\text{m}] = \frac{10^{11}}{3\sqrt{n_p\,[\text{cm}^{-3}]}}$, reducing the plasma density increases λ_p but weakens the plasma response and enhances beam loading. A compromise is therefore necessary. In this work, the first chicane is set to $R_{56} = 0.4$ mm (2.4 m long), and the APD operates at $n_p = 1.3 \times 10^{17}$ cm^{-3} with a length of 2.34 mm. At the APD exit, the energy jitter is reduced to about 0.08%, while beam-loading-induced nonlinearity increases the average relative energy spread to approximately 3.4% (see Table 1).

Table 1: Beam energy parameters after the APD for three representative shots

Central Energy after APD (MeV)	Relative energy jitter (%)	Energy Spread (%)
470.31	-0.02	3.47
470.80	0.08	3.34
470.05	-0.08	3.36

In the downstream section, a similar trade-off arises. A larger negative R_{56} strengthens the chirp and improves energy-spread reduction in the PPD, but excessive bunch lengthening lowers the current and weakens the wakefield, limiting compensation. Considering this balance, the second chicane is set to $R_{56} = -0.7$ mm, and the PPD plasma density to 8.0×10^{14} cm^{-3}.

Table 2: Beam energy parameters after the PPD for three representative shots

Central Energy after PPD (MeV)	Relative energy jitter (%)	Energy Spread (%)
448.01	0.05	0.41
447.57	-0.05	0.42
447.99	0.04	0.46

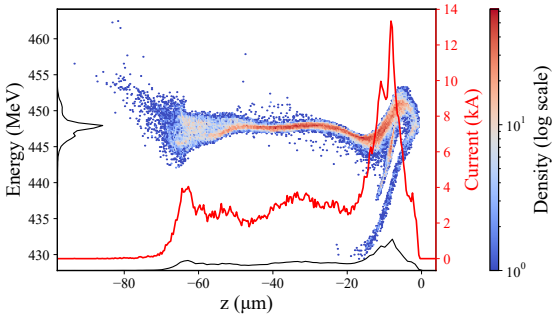

Figure 3: Longitudinal phase space of the beam at the exit of the PPD, showing a significantly reduced correlated energy spread.

After the PPD, the energy spread is significantly reduced. To further improve beam quality, two apertures are used: one between the fourth APL and the PPD to remove particles with large transverse offsets from upstream chromatic and dispersive effects, and another at the PPD exit to eliminate particles outside the channel radius. With these apertures, the energy spread decreases to about 0.4% (see Table 2), with a transmission of 82%. The corresponding longitudinal phase space is shown in Fig. 3.

TRANSPORT TO HEPS BOOSTER

After the energy spread and energy jitter are reduced to the required range, the beam is transported to the HEPS booster through a dedicated beamline. The design focuses on matching the beam optics to the booster acceptance while preserving beam quality.

Table 3: Optics matching between the transport line and the HEPS booster. 't' ('b') denotes the transport line exit (booster injection point)

β_x(t/b) (m)	β_y(t/b) (m)	α_x(t/b) –	α_y(t/b) –	η_x(t/b) (m)
13.7/13.7	15.0/15.0	0.0/0.0	0.0/0.0	0.0/0.0

The optics are optimized to match the Twiss parameters and dispersion at the injection point (see Table 3). The transport line consists of dipoles and quadrupoles for beam steering and focusing (see Fig. 1). Beam loss along the transport line is negligible.

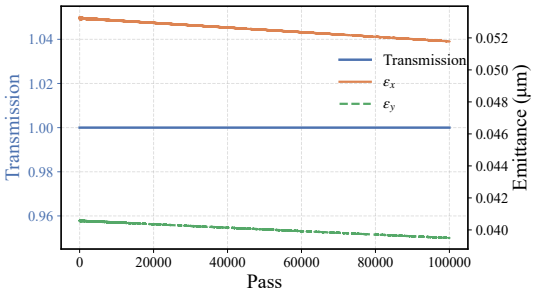

Figure 4: Beam transmission in the HEPS booster, demonstrating nearly loss-free injection.

The beam is then injected into the HEPS booster, which is simulated using the code `elegant` in particle tracking mode. The transmission in the booster is maintained at approximately 100% (see Fig. 4), indicating that the beam parameters are compatible with the injection requirements, while no noticeable transverse emittance growth is observed.

The beam dynamics are further characterized in phase space after 1.0×10^5 turns. Both longitudinal and transverse phase spaces are examined, as shown in Fig. 5. The results indicate that the t–p, x–x', and y–y' phase spaces remain well preserved, with no significant dilution or filamentation observed, confirming stable six-dimensional beam dynamics in the booster.

CONCLUSIONS AND DISCUSSION

A plasma-based scheme for stabilizing nC-level LPA beams has been proposed, combining magnetic chicanes with the APD and the PPD to simultaneously control energy jitter and energy spread under strong beam loading. By optimizing the upstream R_{56} together with the APD density, and employing a downstream negative-R_{56} chicane and low-density PPD, correlated energy spread is effectively suppressed. Transverse apertures further improve beam quality.

Start-to-end simulations show that a 1 nC beam with initial $\pm 2\%$ energy jitter and 1.2% energy spread can be reduced to $\pm 0.05\%$ and 0.4%, with 82% transmission. A matching transport line to the HEPS booster is designed. `elegant` tracking indicates nearly 100% injection efficiency and stable beam dynamics, confirming the feasibility of nC-level LPA beams for booster injection.

ACKNOWLEDGEMENTS

The authors would like to thank Mr. Zihang Zhao and Mr. Liyan Qin from IHEP for their valuable comments and suggestions.

REFERENCES

[1] T. Tajima and J. M. Dawson, "Laser electron accelerator", *Phys. Rev. Lett.*, vol. 43, no. 4, pp. 267–270, Jul. 1979. doi:10.1103/PhysRevLett.43.267

[2] V. Malka *et al.*, "Electron acceleration by a wake field forced by an intense ultrashort laser pulse", *Science*, vol. 298, no. 5598, pp. 1596–1600, Nov. 2002. doi:10.1126/science.1076782

[3] W. P. Leemans *et al.*, "GeV electron beams from a centimetre-scale accelerator", *Nature Physics*, vol. 2, pp. 696–699, Sep. 2006. doi:10.1038/nphys418

[4] I. Blumenfeld *et al.*, "Energy doubling of 42 GeV electrons in a metre-scale plasma wakefield accelerator", *Nature Physics*, vol. 445, pp. 741–744, Feb. 2007. doi:10.1038/nature05538

[5] M. Litos *et al.*, "High-efficiency acceleration of an electron beam in a plasma wakefield accelerator", *Nature*, vol. 515, pp. 92–95, Nov. 2014. doi:10.1038/nature13882

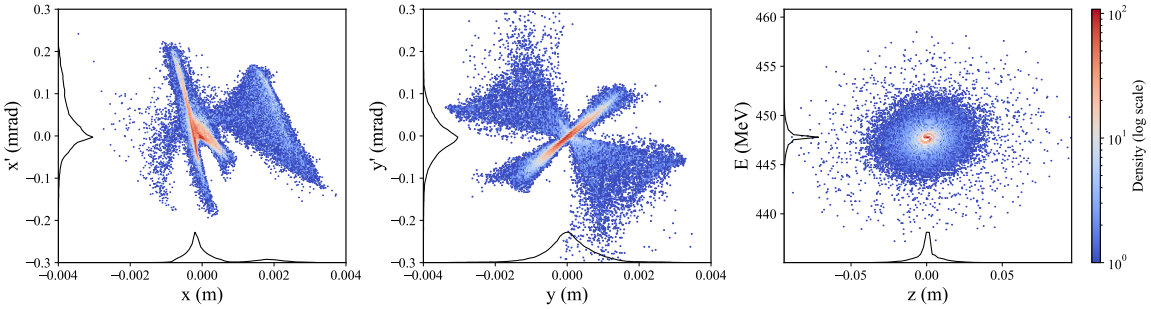

Figure 5: Longitudinal (t–p) and transverse (x–x', y–y') phase spaces after 1.0×10^5 turns in the HEPS booster, showing stable six-dimensional beam dynamics and preserved phase-space structure.

[6] S. Corde *et al.*, "Multi-gigaelectronvolt acceleration of positrons in a self-loaded plasma wakefield", *Nature*, vol. 524, pp. 442–445, Aug. 2015. doi:10.1038/nature14890

[7] O. Lundh, J. Lim, C. Rechatin, *et al.*, "Few femtosecond, few kiloampere electron bunch produced by a laser–plasma accelerator", *Nature Physics*, vol. 7, pp. 219–222, 2011. doi:10.1038/nphys1872

[8] E. Brunetti *et al.*, "Low emittance, high brilliance relativistic electron beams from a laser-plasma accelerator", *Phys. Rev. Lett.*, vol. 105, no. 21, p. 215007, Nov. 2010. doi:10.1103/PhysRevLett.105.215007

[9] G. R. Plateau *et al.*, "Low-emittance electron bunches from a laser-plasma accelerator measured using single-shot x-ray spectroscopy", *Phys. Rev. Lett.*, vol. 109, no. 6, p. 064802, Aug. 2012. doi:10.1103/PhysRevLett.109.064802

[10] G. Golovin, S. Banerjee, C. Liu, *et al.*, "Intrinsic beam emittance of laser-accelerated electrons measured by x-ray spectroscopic imaging", *Scientific Reports*, vol. 6, p. 24622, 2016. doi:10.1038/srep24622

[11] R. Weingartner *et al.*, "Ultralow emittance electron beams from a laser-wakefield accelerator", *Phys. Rev. Spec. Top. Accel. Beams*, vol. 15, no. 11, p. 111302, Nov. 2012. doi:10.1103/PhysRevSTAB.15.111302

[12] W. van Dijk, J. M. Corstens, S. B. van der Geer, M. J. van der Wiel, and G. J. H. Brussaard, "Effects of timing and stability on laser wakefield acceleration using external injection", *Phys. Rev. Spec. Top. Accel. Beams*, vol. 12, no. 5, p. 051304, May 2009. doi:10.1103/PhysRevSTAB.12.051304

[13] J. Faure *et al.*, "A laser-plasma accelerator producing monoenergetic electron beams", *Nature*, vol. 431, pp. 541–544, Sep. 2004. doi:10.1038/nature02963

[14] A. Buck *et al.*, "Shock-front injector for high-quality laser-plasma acceleration", *Phys. Rev. Lett.*, vol. 110, no. 18, p. 185006, May 2013. doi:10.1103/PhysRevLett.110.185006

[15] Y. P. Wu *et al.*, "Near-ideal dechirper for plasma-based electron and positron acceleration using a hollow channel plasma", *Phys. Rev. Appl.*, vol. 12, no. 6, p. 064011, Dec. 2019. doi:10.1103/PhysRevApplied.12.064011

[16] A. F. Pousa *et al.*, "Energy Compression and Stabilization of Laser-Plasma Accelerators", *Phys. Rev. Lett.*, vol. 129, no. 9, p. 094801, 2021. doi:10.1103/PhysRevLett.129.094801

[17] X. Y. Shi and H. S. Xu, "Design of an LPA-Based First-Stage Injector for a Synchrotron Light Source", in *Proc. IPAC'22*, Bangkok, Thailand, Jun. 2022, pp. 1639–1643. doi:10.18429/JACoW-IPAC2022-WEOZGD1

[18] X. Shi, H. Xu, D. Li, J. Wang, and M. Zeng, "Energy stabilization of high-charge bunches from laser plasma accelerators", *New J. Phys.*, vol. 26, no. 7, p. 073045, Jul. 2024. doi:10.1088/1367-2630/ad6634